Electronic supplementary material for "Silent but deadly? Physics says seldom, memory says mostly"

Chan Young Joe
Independent Researcher, Incheon, Republic of Korea

Contents

S1 Odorant chemistry **1**

S2 Acoustics **3**

S3 CFD validation **4**

S4 CFD scenes **5**

S5 Scene doses **7**

S6 Scene weights **8**

S7 Robustness of the headline **8**

S8 Breath sampling **8**

S9 Origin of the odorants **8**

S10 Cross-cultural survey **10**

S11 Code and data **11**

S12 Parameters **11**

S1 Odorant chemistry

S1.1 Methods

Odour activity. Each sulfur gas contributes an odour activity value (OAV), its mole fraction over its detection threshold, $\mathrm{OAV}_i = x_i/\theta_i$. The passage's OAV is their sum; we assume additivity and do not model mixture suppression. We compare two measured compositions:

- 87 passages of 16 volunteers [S1], used throughout the dispersion model;
- 28 passages measured by gas chromatography: H_2S 149, methanethiol 216 and dimethyl sulfide 144 $\mathrm{nmol\,L^{-1}}$ [S2].

Three threshold sets bracket the observer: a trained panel [S3]; population values, the geometric means of detection thresholds for H_2S and methanethiol [S4] and, for dimethyl sulfide, the median recognition threshold of an untrained panel of 35 [S5]; and the lowest values in Verschueren's handbook, as tabulated in ref. S2.

Removal check. Zinc acetate precipitates H_2S and thiols; activated charcoal adsorbs all three gases. For both treatments, ref. S1 reports the gas concentrations and two judges' ratings before and after. We predict the rating ratio as $(\mathrm{OAV_{after}}/\mathrm{OAV_{before}})^n$ with $n = 0.20$–0.45, an assumed bracket around the 0.28 measured for canine flatus [S6], without fitting.

Buoyancy. The reduced gravity $g' = g(\rho_a - \rho_g)/\rho_a$ of each of 16 measured compositions [S7] is split into a thermal part, $g(1-T_a/T_g)$, for gas at 37 °C in air at 22 °C, and a compositional part, $g(M_a - M_g)/M_a$, at equal temperature with air at 50% relative humidity. The water-vapour content of flatus has not been measured, so we bracket dry and saturated gas.

Gas-phase and surface losses. Gas-phase losses use IUPAC rate constants at 298 K for reaction with OH, O_3, NO_3 and Cl [S8], with oxidant levels measured in an office: OH 0.6–$9.8 \times 10^5\,\mathrm{cm^{-3}}$ and O_3 0.7–2.6 ppb (daily means) [S9]. Two assumed upper cases add OH $10^6\,\mathrm{cm^{-3}}$ with O_3 40 ppb, and Cl $10^6\,\mathrm{cm^{-3}}$ during hypochlorite cleaning. No deposition velocity v_d has been published for these gases on indoor surfaces, so surface loss is bracketed as $k = v_d\,S/V$ with $S/V = 3\,\mathrm{m^{-1}}$.

Dilution in a panel test. Ref. S2 reports the lowest source concentration that every panel member detected when 100 mL was released below the nose. Divided by a detection threshold, it gives the dilution between release and nose in that test, which we compare with the breath-averaged dilution of the analytic model.

S1.2 Results

Which molecule. Over the two measured compositions and three threshold sets, methanethiol carries 43–94% of the summed OAV and never less than H_2S (Figure S1a).

- With the composition of ref. S1, methanethiol and H_2S carry about equal shares (43–54% and 43–46% with trained-panel and population thresholds). Methanethiol is one fifth as concentrated, but its threshold is 5–6 times lower.
- With the composition of ref. S2, or with the lowest reported thresholds, methanethiol carries 60–94%.

The two datasets disagree on the concentrations themselves: H_2S is five times methanethiol in one and slightly below it in the other, a difference ref. S2 attributes to the bean-rich diet of the first. In that study's panel test, gas mixtures with methanethiol above its flatus threshold smelled like most passages.

Composition does not enter the silent/audible comparison: transport is linear and acts on all three gases alike, so every ratio is the same for any composition. Absolute OAVs are 11–38% lower with the second composition.

The intensity law with real flatus. Zinc acetate lowers the summed OAV by a factor of 14. Stevens' law then predicts rating ratios of 0.31–0.59, and the two judges gave 0.28 and 0.59 [S1]. Activated charcoal lowers the OAV about 260-fold and is rated far weaker than the power law predicts, as power laws fail near threshold. The silent/audible comparison uses supra-threshold ratios, where the law held.

What makes a passage rise or sink. Composition sets most of the buoyancy (Figure S1b).

- For the median passage the compositional part of the reduced gravity ($+1.25\,\mathrm{m\,s^{-2}}$ dry, +1.40 saturated) is about three times the thermal part (+0.47).
- H_2 and CH_4 make flatus light and CO_2 makes it heavy; the compositional part falls with CO_2 content ($r = -0.80$).
- 6–12% of passages sink even while hot. After cooling to room temperature, 25–38% are heavier than air.

Table S1: Gas-phase lifetime of the odorants and the fraction lost in 120 s. Office oxidant levels are measured [S9]: low, OH 0.6×10^5 cm^{-3} and O_3 0.7 ppb; high, OH 9.8×10^5 cm^{-3} and O_3 2.6 ppb (the highest daily means of each, measured on different days). The cleaning case assumes Cl 10^6 cm^{-3}. Rate constants from ref. S8.

scenario	H_2S	CH_3SH	DMS
office, low	40 d / 0.003%	5.7 d / 0.03%	28 d / 0.005%
office, high	2.5 d / 0.06%	8.6 h / 0.4%	1.8 d / 0.08%
hypochlorite cleaning	3.5 h / 0.9%	1.2 h / 2.8%	0.8 h / 4.0%

The dispersion model uses these signed values of g'.

Losses on the way to the nose (Table S1).

- In an office, gas-phase oxidation removes at most 0.4% of any of the three gases in 120 s, and hypochlorite cleaning less than 4%.
- Surface deposition is unconstrained by data. It removes 0.7% in 120 s at $v_d = 0.002$ cm s^{-1} and 51% at 0.2 cm s^{-1}. Treating the odorants as passive scalars therefore holds against chemistry by two to three orders of magnitude, and against deposition only if $v_d \lesssim 0.01$ cm s^{-1}.
- Deposition would remove most from the silent release, which stays close to the body and the seat, and would lower its doses further in the simulated scenes.

How dilute a passage arrives. The panel test of ref. S2 implies a dilution of 0.6–13 $\times 10^4$ between release and nose, depending on the threshold set. The breath-averaged dilution of the analytic model at the neighbour has a median of 1.8×10^3 (10–90%: 2.5×10^2–2.9×10^4). The panel value is biased upwards, because it requires the least sensitive panellist to detect but divides by the thresholds of the most sensitive. The analytic model is at the concentrated end of the panel range, as intended for an upper bound, and within about an order of magnitude of it.

Composition and volume. Larger passages contain more fermentation gas and less nitrogen (per passage, $r = +0.56$ for CO_2 and -0.50 for N_2, $n = 87$), while the sulfur concentrations do not change with volume ($|r| \leq 0.22$, not significant); sulfur mass therefore rises with passage volume [S7]. At high production rates almost all flatus is fermentation gas [S10]. Under bean, fibre, fruit and lactulose challenges the fermentation-gas fraction rises with output ($r = +0.86$ to $+0.98$ across diet or treatment means, computed from the published tables [S11–S16], for ref. S13 from the 12 control and bean rows without silicone; in one person from 26% at 55 mL to 79% at 720 mL per 4 h [S17]). One study is an exception: on an ordinary diet the fraction did not rise with output ($r = -0.41$ across 20 subjects), and after brussels sprouts the extra gas was mostly nitrogen [S18]. The density of the gas does not follow the amount: carbon dioxide and hydrogen rise together, and the mean molar mass, 22–32 g mol^{-1} across diets, is set by the substrate's CO_2:H_2 ratio (its correlation with output ranges from -0.37 to $+0.90$ across seven studies). Composition therefore cannot link audibility to the amount of gas, since it enters audibility only through density (Section S2).

S2 Acoustics

Duration and orifice. Flatus passes during an anal relaxation lasting 19 ± 6 s [S19] (relaxations accompanying pan-colonic pressurizations last 23 ± 4 s [S20]), which bounds the duration T from above, and the mid anal canal widens to about 8 mm only at balloon pressures (40–55 mmHg)

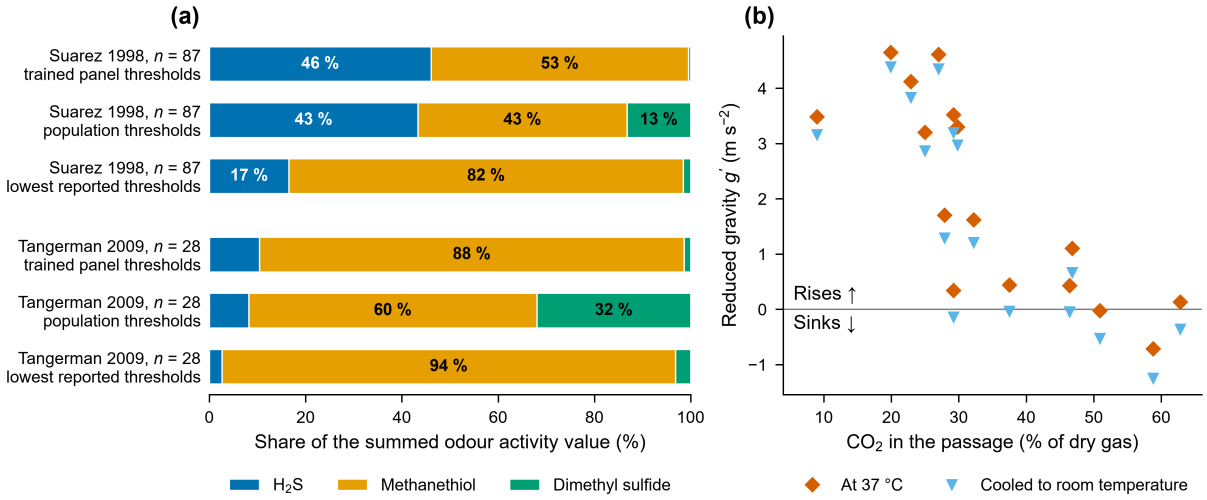


Figure S1: Odorants and buoyancy. (a) Share of the summed OAV carried by H_2S, methanethiol and dimethyl sulfide, for two measured compositions [S1, S2] under three threshold sets. (b) Reduced gravity of 16 measured compositions [S7] against their CO_2 content, at 37 °C (dry basis; water saturation shifts these values by -0.04 to $+0.29\,\mathrm{m\,s^{-2}}$) and after cooling to room temperature.

[S21, S22] above the rectal pressures at which flatus usually passes (median rise 8 mmHg, range −10 to 88) [S23], which bounds the effective diameter d.

Valve. The anal canal is modelled as a lip reed, a soft-tissue valve that self-oscillates in the flow through it, as the lips do on a brass instrument. It oscillates when the driving pressure $\frac{1}{2}\rho(u_0/C_\mathrm{d})^2$ exceeds a threshold $P_\mathrm{th} = 0.6$–2.5 kPa (nominal 1.2 kPa), with discharge coefficient $C_\mathrm{d} = 0.85$. The closest measured soft-tissue sphincter source, the pharyngo-oesophageal segment that drives oesophageal and tracheo-oesophageal speech, phonates at 1.1–2.5 kPa: sustained phonation from 1.1 kPa [S24], 1.8 kPa below the segment at minimum loudness [S25] and about 2.5 kPa on average during speech (individuals 1.0–3.0 kPa) [S26]. This bounds the onset from above; lips on a brass instrument start at about 0.6 kPa [S27]. This gives an onset velocity $u_\mathrm{onset} \approx 42\,\mathrm{m\,s^{-1}}$ (21–71).

An oscillating valve radiates as a harmonic monopole with harmonics falling by 12 dB per octave. Its fundamental is taken as 160 Hz (60–300 Hz), between oesophageal and tracheo-oesophageal speech at 60–150 Hz [S24, S28–S30] and recordings of flatus near 270 Hz, which are not peer-reviewed [S31]. A release counts as *audible* when at least one harmonic exceeds both the ISO 226 hearing threshold [S32] and the masked threshold of the background, computed from the critical ratio [S33]. Backgrounds range from a 35 dB(A) living room to a 77 dB(A) subway car.

Valve state. Manometry shows flatus passing through a relaxed sphincter, at a median rectal pressure rise of 8 mmHg (range −10 to 88; 0–15 mmHg when flatus is only sensed) [S23], with a fall in anal pressure [S19], but also against a contracted sphincter [S34]. The 85% silent share treats the onset pressure as a property of the tissue and does not distinguish the two.

S3 CFD validation

- *Free round jet* (axisymmetric, Re = 6700, three meshes). The velocity-decay constant is 5.0 and the scalar constant $K_c = 4.3$–4.6, with a grid uncertainty of at most 3.7%. The k–ω SST model spreads round jets about 25% too fast, which over-dilutes audible releases by about 15% and so favours the silent release.

Table S2: Representative releases: median and 90th percentile of the exit momentum flux within each class.

release	class	V (mL)	T (s)	d (mm)	u_0 ($\mathrm{m\,s^{-1}}$)	M_0 ($\mathrm{m^4\,s^{-2}}$)
S50	silent	122	4.76	3.06	3.5	8.9×10^{-5}
S90	silent	66	0.65	2.45	22	2.2×10^{-3}
A50	audible	86	0.42	1.67	94	1.9×10^{-2}
A90	audible	279	0.34	2.54	162	0.13

- *Convective boundary layer* of a simplified seated manikin with skin at 33 °C, compared with thermal-manikin data [S35]. The face-front peak velocity is 40–56% too high at room temperatures of 20–26 °C; its change with room temperature is reproduced (−27% against −33% measured).

- *Near-body source to breathing zone.* The chamber of ref. S36 ($4.6 \times 4.6 \times 2.36$ m, $115\,\mathrm{m^3\,h^{-1}}$ through two ceiling supplies, exhaust at 1.8 m) with the scene manikin, chair, skin temperature and solver; a $3.5\,\mathrm{L\,min^{-1}}$ source between the thighs at 0.5 m runs for 10 min. Intake fraction $\mathrm{iF} = Q_\mathrm{b} \int C_\mathrm{bz}\,\mathrm{d}t/m$ with $Q_\mathrm{b} = 0.5\,\mathrm{m^3\,h^{-1}}$, from the breathing-zone probe at 1.1 m; after 22 min the room-mean level decays at the measured air-exchange rate. Result 8.1, 9.1 and 11.0 per mille over 10, 22 and 100 min against 5.5, 7.7 and 9.8 measured; relative to the well-mixed room 11.0 and 2.6 against 7.4 and 2.3. The manikin's convective output is 79 W. Supply direction, supply temperature and exhaust size are not reported and were assumed (downward, room temperature, 0.3 m square).

- *Mesh.* The median silent release alone on the sofa mesh and on a mesh refined by 1.5 in every direction (0.72 and 2.2 million cells, same refinement levels): 150-s worst breath 0.42 and 1.28 at the releaser, 0.17 and 0.094 at the neighbour. Released fourth in the four-release run on the base mesh, the same passage gives 0.33 and 0.071, so the release order matters about as much as the mesh.

- *Well-mixed tail.* Two coupled 10-minute runs of the sofa (one silent, one audible 92-mL release): the tail predicts 1.00 and 0.67 (silent: releaser, neighbour) and 0.84 and 0.71 (audible) of the actual worst breath at 600 s. The neighbours' level keeps creeping up after 300 s; nothing worse arrives later.

S4 CFD scenes

All scenes use the solver of the main text, skin at 33 °C and walls at 23 °C. Each runs 90 s without a release; the four representative releases then follow 30 s apart (strongest first) on separate scalars, each until 150 s after its start. A release enters behind the releaser's buttocks, pointing down and back, through a 1 cm-radius inlet that carries its momentum flux and odorant flux (audible releases are pre-diluted with room air to fit the inlet), with the flatus buoyancy ($g' = 1.70\,\mathrm{m\,s^{-2}}$) as an equivalent temperature excess.

- *Sofa.* A $3.2 \times 3.2 \times 2.6$ m living room with a 0.5 m ceiling vent for pressure relief (size and position assumed). Two seated manikins sit 0.6 m apart on a two-seat sofa whose base is solid to the floor. Mesh 0.72 million cells, 1 cm on the bodies and 2.5 mm on the inlet face. Two variants rotate the releaser's upper body about the hip: reclined by 4.5 °, so that the back closes onto the backrest, and leaning forward by 10 °, so that the gap behind the back opens.

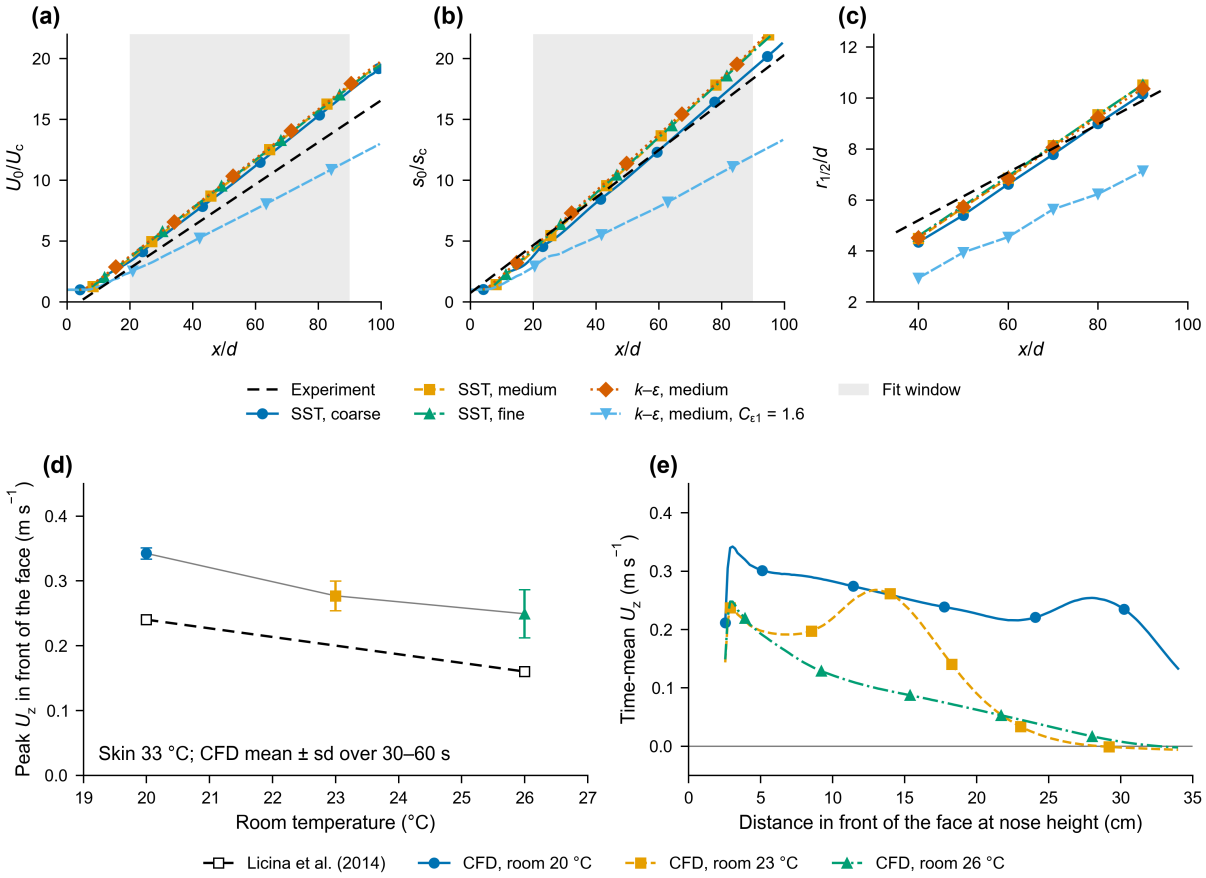


Figure S2: Validation. Top: free round jet at Re = 6700, k–ω SST on three meshes and two k–ε variants, against the experimental correlations: (a) centreline velocity decay, (b) centreline scalar decay, (c) half-width (the experiment gives only the spreading rate, 0.094, drawn through the mean of the fine-mesh points); grey: the fit window. Bottom: (d) face-front peak upward velocity of the seated manikin against thermal-manikin data [S35] at 20–26 °C, (e) time-mean vertical velocity profiles at nose height.

Table S3: Worst-breath OAV over 150 s (trained-panel thresholds, volumes as emitted, mean flow).

scene	nose	S50	S90	A50	A90
sofa, upright	releaser	0.33	6.6	6.3	49
	neighbour	0.071	0.090	0.16	17
sofa, reclined 4.5 °	releaser	0.26	20	2.1	25
	neighbour	0.12	0.95	0.95	19
sofa, forward 10 °	releaser	0.49	1.2	0.51	22
	neighbour	0.30	0.26	0.29	36
sofa, upright, trousers	releaser	5.0	1.0	64	110
	neighbour	0.11	0.070	1.0	43
standing, still	releaser	0.13	0.85	0.26	1.9
	neighbour	0.0056	0.0016	0.0004	0.0022
standing, still, trousers	releaser	0.042	0.070	13	40
	neighbour	0.014	0.014	0.0033	0.017
standing, ventilated	releaser	0.38	2.8	15	6.9
	neighbour	0.17	0.049	0.018	0.034
standing, ventilated, trousers	releaser	0.16	22	39	20
	neighbour	0.15	0.066	0.099	0.56
lift	releaser	7.3	2.0	2.9	15
	beside	2.3	1.2	2.1	7.3
	behind	260	26	34	36
	diagonal behind	6.5	2.8	4.8	22

- *Lift.* The car of a 630 kg, eight-person lift, 1.10 m wide, 1.40 m deep and 2.10 m high. Four standing manikins (nose at 1.59 m) stand in a 2×2 grid facing the door; the fan is off, and a 0.2 m ceiling opening relieves pressure (size assumed). Mesh 0.91 million cells. The releaser stands in the front row.
- *Standing pair.* The sofa room without the sofa, with two standing manikins face to face, noses 1.0 m apart. Ventilation is one square ceiling diffuser above the pair supplying $21.2\,\mathrm{L\,s^{-1}}$, 2.9 air changes per hour (EN 16798-1 Category II for two people in a low-polluting $10\,\mathrm{m^2}$ room [S37]), leaving along the ceiling at an assumed $1.5\,\mathrm{m\,s^{-1}}$ and exiting through a ceiling grille.
- *Trousers.* A porous shell 1 cm thick, 2 cm from the skin over pelvis and thighs, open at the waist and hems, with a Darcy resistance from the air permeability of denim ($0.03\,\mathrm{m\,s^{-1}}$ at 100 Pa, EN ISO 9237).
- *Large-eddy simulation.* The upright sofa, bare and in trousers: WALE model, maximum Courant number 0.8, 60 s of spin-up from the RANS flow, then six releases 30 s apart (S50, A50, S90, A90 and the two medians again), each followed for 90 s.

S5 Scene doses

Table S3 lists the 150-s worst-breath OAV of every representative release at every nose (volumes as emitted, RANS). No silent release reaches a sofa or standing neighbour above the trained-panel threshold; in the lift every nose passes it, the person behind the releaser most of all.

S6 Scene weights

Weights are the hours per day an adult spends close to another person in each setting, with passages spread uniformly over waking hours: sofa 1.4 h (television with others in the room, from the American Time Use Survey; bounds 0.8–2.0), lift 0.01 h (four shared rides of about 24 s on working days; 0.0005–0.1) and standing conversation 0.5 h (0.2–1.5, an assumption from the talking and standing shares of the day), i.e. 0.73, 0.005 and 0.26. The home-centred bound takes the high sofa and low lift and standing values, the office-centred bound the reverse. Sources and derivation are in the repository (`refs/scene_weights_sources.md`). Within a scene, postures and ventilation variants count equally.

S7 Robustness of the headline

Bystanders, bare, frequency-weighted; silent worse / audible worse (%), attentive observer unless stated.

- *Scene weights:* central 0.5 / 6.9; home 0.5 / 8.4; office 1.1 / 3.9; equal per scene 7.6 / 9.9. Remembered silent worse 88.4, 91.2, 81.5 and 79.8%.
- *Psychometric tail:* slope 1–4 binary steps (attentive) or 2–5 (distracted), logistic tail, zero detection below the trained-panel threshold, or deterministic detection at it: audible-to-silent ratio 4.2–25 (1.2–86 with the home and office bounds); remembered silent worse 62–98%.
- *Peak factor* (large-eddy over RANS worst breath, 60 s, releases with RANS OAV ≥ 0.01): silent 2.2 (1.0–6.6, $n = 6$), audible 1.3 (0.27–64, $n = 12$); applied by class 1.2 / 8.2. Two realisations of the same release differ by up to a factor of 20, so the factor is a distribution. The smallest silent-only factor that reverses the order is 14 (office bound 5.7); a uniform factor never does (tested to 10^4). The adverse pairing (6.6 silent, 0.27 audible) gives 3.6 / 2.3, with 98% remembered silent worse.
- *Mesh:* silent doses $\times 0.55$ give 0.26 / 6.9, $\times 3.0$ give 1.6 / 6.8.
- *Clothing:* 70% of passages clothed 0.06 / 9.3; 85% 0.06 / 10.2; all 0.06 / 11.1 (sofa upright and standing only).
- *Releaser:* 4.6 / 17.9 (no selection: memory equals physics).

S8 Breath sampling

An audible puff reaches the neighbour after a median of 16 s and passes with a time scale of about 3.9 s (10–90%: 1.5–12 s). Without a warning, the breathing phase barely matters: for a median passage the worst breath captures 81–99% of the peak. A listener warned by the sound needs about 25 s of breath-hold for an even chance of missing the puff (worst breath below 10% of the peak); 33 s, the typical maximum at end-expiration, gives 62%.

S9 Origin of the odorants

Two facts the transport model takes as given have chemical explanations in the literature; we did not test them.

Why sulfur concentration does not follow volume.

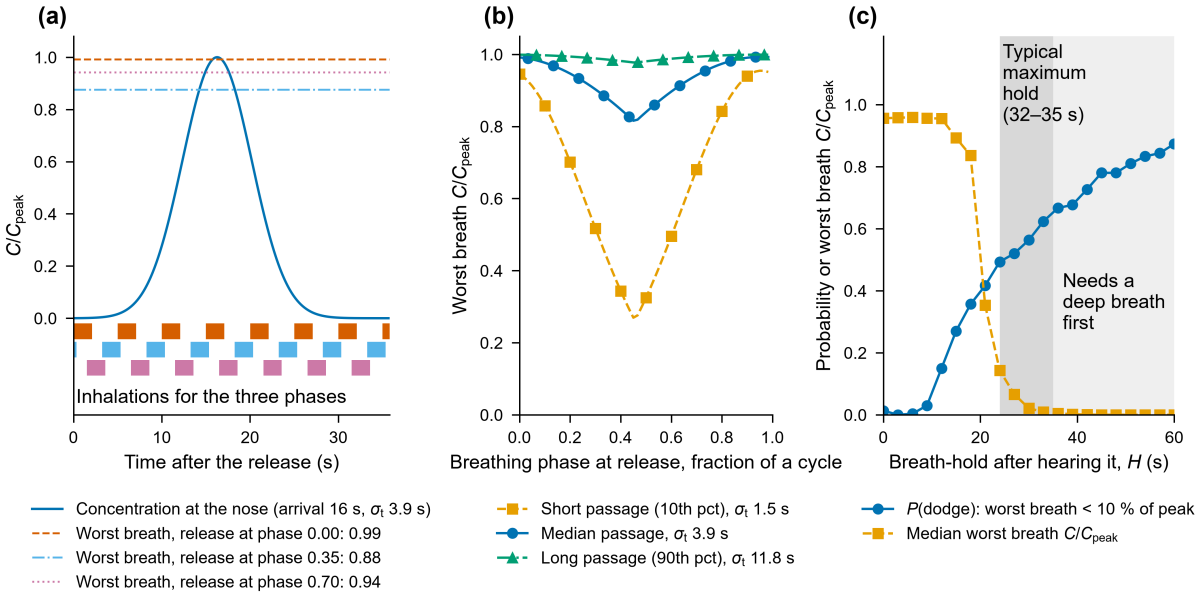


Figure S3: Breath sampling at the neighbour's nose for audible releases. (a) A typical puff (arrival 16 s, passage time scale 3.9 s) and the inhalations of three breathing phases, with the worst breath of each. (b) Without warning: worst breath relative to the peak against the breathing phase at release, for short, median and long passages. (c) Warned: probability of missing the puff (worst breath below 10% of the peak) and median worst breath, against the breath-hold duration after hearing the release (0.5 s reaction latency).

- H_2S comes from sulfate-reducing bacteria [S38] and from cysteine degradation, whose genes are widespread in the gut microbiome [S39]. Sulfate reducers and methanogens both consume H_2, but whether they exclude each other is disputed. Sulfidogenic gut contents produced no methane in some studies [S38, S40], whereas faecal sulfide did not differ between methane producers and non-producers in others [S41, S42], H_2S release from incubated faeces did not correlate with methane release ($r = 0.11$) [S43], and methanogenic faeces suppressed sulfide production sixfold in co-incubation [S44].

- The caecal mucosa of rats removes both gases quickly: methanethiol is demethylated to H_2S, and H_2S is oxidised mainly to thiosulfate [S45]. Rhodanese is the main detoxifying enzyme in human colon [S46], and SELENBP1 oxidises methanethiol with an apparent K_m of 4.8 nM [S47].

- Only free sulfide can enter the gas, and it is less than 5% of faecal total sulfide (free methanethiol is 22–54% of the total) [S2].

The odorants are thus trace products held at a balance of production and fast consumption, whereas passage volume is set by N_2, CO_2, H_2 and CH_4. We infer that this is why sulfur concentration and passage volume are uncorrelated [S7]. Diet moves the balance: a meat-rich diet raised faecal sulfide from 0.22 to 3.38 mmol kg^{-1} in five volunteers [S48], although faecal sulfide reflects the binding capacity of the stool as much as sulfide production [S49], and the response to animal and plant diets differs between people [S50].

Diet can make large passages less sulfurous. Within one diet, sulfur concentration does not change with passage volume (Section S1); across diets it can. In faecal incubations, rapidly fermented fibres produced up to 50 times more gas than poorly fermented fibre while suppressing H_2S by up to 89%, and cysteine raised H_2S 16-fold [S51]. Dietary sulfate tripled sulfide production and cut methane production fivefold, at unchanged stool weight and transit, in three of six subjects [S52]; in the sulfidogenic gut contents of one autopsy subject, H_2S took the place of the

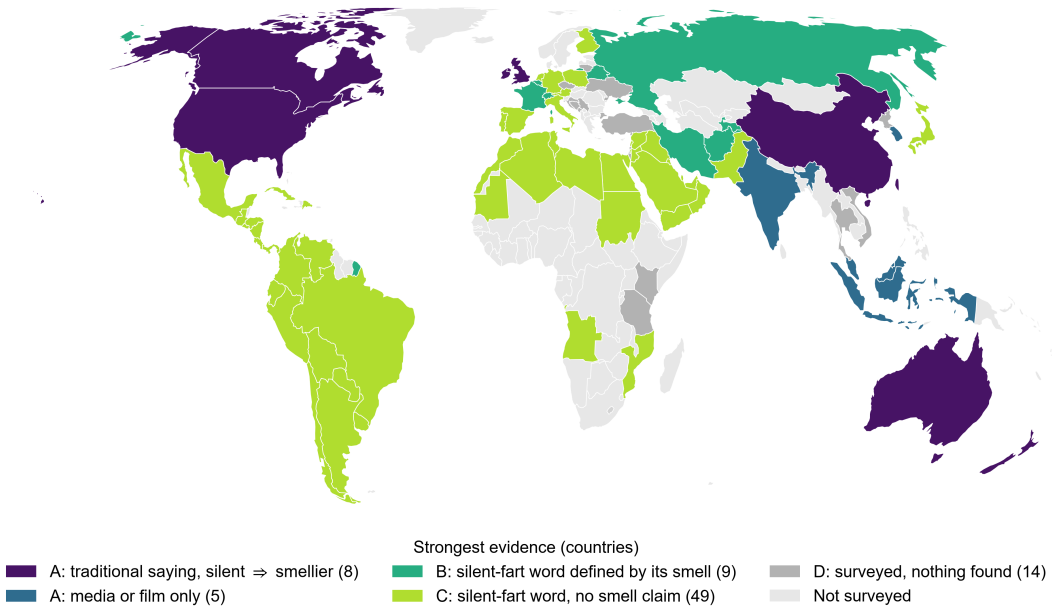


Figure S4: The belief across languages, by evidence level. Each country takes the strongest level among its surveyed languages. A: an explicit saying that silent passages smell worse (traditional, or in media or film only); B: a dedicated word for a silent passage defined by its smell; C: a dedicated word with no smell claim; D: surveyed, nothing found. Documentary presence is not prevalence; historical languages are not mapped. Borders: Natural Earth 1:110m.

CH_4 found in a methanogenic one [S40], diverting hydrogen from gas volume to sulfide [S53]. Interventions aimed at sulfur move sulfur alone: bismuth cut faecal H_2S release 23-fold with total gas unchanged [S54], and charcoal, yucca and zinc acetate cut H_2S production by 38–86% without changing gas production in dog faecal incubations, and fed to dogs did not change the number of emissions [S55]. Because audible passages are larger, a diet-driven link of this kind would make audible passages less sulfurous per millilitre, in the direction of the belief. Its size in vivo is unknown: no study has measured sulfur gases and flatus volume together across diets.

Why methanethiol smells foul. The human receptor OR2T11 responds to short thiols, including methanethiol, in a copper-dependent way, but did not respond to H_2S in that assay [S56]. Human nasal mucus contains about 2.5 µM copper [S57], below the 30 µM added in the receptor assays, so the receptor's role in vivo is plausible but not shown. Other receptors respond to sulfur ligands without copper [S58–S60]. A receptor that responds to methanethiol and not to H_2S would make methanethiol the characteristic note of flatus independently of thresholds; we infer this, it has not been tested.

S10 Cross-cultural survey

We searched dictionaries, proverb collections and etymological handbooks in 32 languages or historical stages for a dedicated word for a silent passage and for an explicit claim that it smells worse, and checked every entry used against a retrieved source. Each language is graded by its strongest evidence: A, an explicit saying (traditional, or in media or film only); B, a dedicated word defined by its smell; C, a dedicated word without a smell claim; D, nothing found. The silent/loud distinction is lexicalised in at least five language families. The explicit claim is traditional only in Chinese and English, and smell-defined silent words arose independently at least four times within Indo-European. The survey records whether the belief is documented in a language, not how many speakers hold it.

S11 Code and data

Code, inputs and processed outputs are in the repository named in the Data accessibility statement of the main text; its `README.md` lists the source files of every result. They are not duplicated here.

S12 Parameters

Table S4: Model parameters: nominal value, range sampled or tested, and basis: taken from a cited measurement, derived from cited data, partly sourced, taken from a non-peer-reviewed source, or assumed. Parameter names are those of the code; the source and notes for every entry are in `params/params.yaml` of the code archive.

parameter	nominal	range	units	basis
Source				
`T_gas`	310.15	309.85–310.65	K	measured
`V_passage`	9.2×10^{-5}	1.7×10^{-5}–3.75×10^{-4}	m^3	derived
`V_daily`	7.05×10^{-4}	4.76×10^{-4}–1.49×10^{-3}	$m^3\,d^{-1}$	measured
`n_daily`	10	1–20	d^{-1}	measured
`d_orifice`	0.004	0.001–0.008	m	partly sourced
`T_release`	1	0.3–20	s	partly sourced
`dp_rectal`	2000	500–4000	Pa	assumed
`p_anal_rest`	8666	6133–12000	Pa	measured
`g_reduced`	1.7	−0.66 to 4.68	$m\,s^{-2}$	derived
`nu_gas`	1.7×10^{-5}		$m^2\,s^{-1}$	assumed
`c_H2S`	1.06	0.26–1.86	$\mu mol\,L^{-1}$	measured
`c_CH3SH`	0.21	0.05–0.37	$\mu mol\,L^{-1}$	measured
`c_DMS`	0.08	0.04–0.12	$\mu mol\,L^{-1}$	measured
`sulfur_sigma_ln`	1.1	1–1.25	–	derived
Odour thresholds				
`H2S`	0.41	0.41–0.9	ppbv	measured
`CH3SH`	0.07		ppbv	measured
`DMS`	3		ppbv	measured
Jet and puff				
`B_u`	5.8	5.8–5.9	–	measured
`S_jet`	0.094	0.094–0.102	–	measured
`K_c`	5.11	4.73–5.2	–	measured
`Gamma_sj`	2.8	2.74–2.86	–	measured
`C_puff`	2.6	2.54–2.66	–	measured
`alpha_th`	0.25	0.15–0.35	–	measured
`alpha_jet`	0.07	0.065–0.08	–	measured
`alpha_plume`	0.12	0.1–0.16	–	measured
Environment				
`u_handoff`	0.15	0.05–0.25	$m\,s^{-1}$	assumed
`u_CBL`	0.17	0.11–0.24	$m\,s^{-1}$	measured
`u_CBL_pelvis`	0.1	0.05–0.15	$m\,s^{-1}$	assumed
`u_own_eff`	0.11	0.07–0.16	$m\,s^{-1}$	derived
`delta_CBL`	0.1	0.05–0.15	m	assumed
`u_room`	0.08	0.03–0.15	$m\,s^{-1}$	assumed
`K_turb`	0.002	1×10^{-4}–0.013	$m^2\,s^{-1}$	partly sourced
`D_H2S_air`	1.65×10^{-5}	1.62×10^{-5}–1.77×10^{-5}	$m^2\,s^{-1}$	partly sourced
Geometry				
`eye_sit_m`	0.804	0.75–0.86	m	measured
`eye_sit_f`	0.748	0.698–0.799	m	measured

Table S4: Model parameters (continued).

parameter	nominal	range	units	basis
`eye_stand_m`	1.64	1.536–1.753	m	derived
`eye_stand_f`	1.517	1.421–1.626	m	derived
`L_own`	0.74	0.65–0.85	m	assumed
`L_neighbour`	1	0.8–1.4	m	assumed
Breathing				
`V_tidal`	6.3×10^{-4}	4×10^{-4}–8.3×10^{-4}	m^3	measured
`f_breath`	12	10–16	min^{-1}	measured
`Ti_Ttot`	0.42	0.34–0.5	–	measured
`T_insp`	2.1	1.6–2.7	s	derived
Acoustics				
`f0_flatus`	160	60–300	Hz	partly sourced
`bg_library`	40	35–45	dB(A)	assumed
`bg_living`	35	30–45	dB(A)	assumed
`bg_office`	45	43–55	dB(A)	measured
`bg_restaurant`	74	67–83	dB(A)	measured
`bg_subway`	77	74–80	dB(A)	measured
`P_th`	1200	600–2500	Pa	partly sourced
`C_d`	0.85	0.6–1	–	partly sourced
`alpha_mod`	0.7	0.5–1	–	assumed
`harm_slope`	−12	−18 to −6	dB/octave	assumed
`n_harm`	8		–	assumed
`A_cloth`	1	0–3	dB	partly sourced
`r_listener`	0.6	0.4–3	m	assumed
Perception and observers				
`n_stevens`	0.28	0.2–0.45	–	measured
`k_w_H2S`	0.95	0.8–1.2	intensity units per decade	partly sourced
`weber_C`	0.28	0.05–0.4	$\Delta C/C$	measured
`tau_adapt`	80	40–120	s	assumed
`a_inf`	0.35	0.25–0.4	–	partly sourced
`sniff_ratio`	0.64	0.61–0.75	–	measured
`t_react`	0.5	0.3–1.5	s	assumed
`H_max`	33	24–90	s	measured
`thr_scale_typ`	0.05	0.05–0.1	–	measured
`thr_sd_bs`	2		binary steps	measured
`distracted_factor`	26		–	measured
`distracted_sd_bs`	3.5		binary steps	measured
`recovery_gain`	1.5	1–2	–	assumed

References

[S1] F. L. Suarez, J. R. Springfield, and M. D. Levitt. Identification of gases responsible for the odour of human flatus and evaluation of a device purported to reduce this odour. *Gut*, 43(1):100–104, 1998. doi:10.1136/gut.43.1.100.

[S2] A. Tangerman. Measurement and biological significance of the volatile sulfur compounds hydrogen sulfide, methanethiol and dimethyl sulfide in various biological matrices. *Journal of Chromatography B*, 877:3366–3377, 2009. doi:10.1016/j.jchromb.2009.05.026.

[S3] Y. Nagata. *Measurement of odor threshold by triangle odor bag method.* Office of Odor, Noise and Vibration, Environmental Management Bureau, Ministry of the Environment, Government of Japan, 2003.

[S4] J. E. Amoore and E. Hautala. Odor as an aid to chemical safety: odor thresholds compared

with threshold limit values and volatilities for 214 industrial chemicals in air and water dilution. *Journal of Applied Toxicology*, 3(6):272–290, 1983. doi:10.1002/jat.2550030603.

[S5] F. V. Wilby. Variation in recognition odor threshold of a panel. *Journal of the Air Pollution Control Association*, 19(2):96–100, 1969. doi:10.1080/00022470.1969.10466466.

[S6] S. B. Collins, G. Perez-Camargo, G. Gettinby, R. F. Butterwick, R. M. Batt, and C. J. Giffard. Development of a technique for the in vivo assessment of flatulence in dogs. *American Journal of Veterinary Research*, 62(7):1014–1019, 2001. doi:10.2460/ajvr.2001.62.1014.

[S7] F. L. Suarez, J. K. Furne, J. Springfield, and M. D. Levitt. Insights into human colonic physiology obtained from the study of flatus composition. *American Journal of Physiology - Gastrointestinal and Liver Physiology*, 272(5):G1028–G1033, 1997. doi:10.1152/ajpgi.1997.272.5.G1028.

[S8] R. Atkinson, D. L. Baulch, R. A. Cox, et al. Evaluated kinetic and photochemical data for atmospheric chemistry: Volume I - gas phase reactions of Ox, HOx, NOx and SOx species. *Atmospheric Chemistry and Physics*, 4:1461–1738, 2004. doi:10.5194/acp-4-1461-2004.

[S9] E. A. Fiorentino, H. Chen, A. Gandolfo, et al. Measurements and Modelling of OH and Peroxy Radicals in an Indoor Environment Under Different Light Conditions and VOC Levels. *Atmospheric Environment*, 292:119398, 2023. doi:10.1016/j.atmosenv.2022.119398.

[S10] J. Tomlin, C. Lowis, and N. W. Read. Investigation of normal flatus production in healthy volunteers. *Gut*, 32(6):665–669, 1991. doi:10.1136/gut.32.6.665.

[S11] F. R. Steggerda and J. F. Dimmick. Effects of Bean Diets on Concentration of Carbon Dioxide in Flatus. *American Journal of Clinical Nutrition*, 19(2):120–124, 1966. doi:10.1093/ajcn/19.2.120.

[S12] F. R. Steggerda. GASTROINTESTINAL GAS FOLLOWING FOOD CONSUMPTION. *Annals of the New York Academy of Sciences*, 150(1):57–66, 1968. doi:10.1111/j.1749-6632.1968.tb19031.x.

[S13] D. H. Calloway and S. E. Burroughs. Effect of dried beans and silicone on intestinal hydrogen and methane production in man. *Gut*, 10(3):180–184, 1969. doi:10.1136/gut.10.3.180.

[S14] A. U. O'Donnell and S. E. Fleming. Influence of frequent and long-term consumption of legume seeds on excretion of intestinal gases. *American Journal of Clinical Nutrition*, 40 (1):48–57, 1984. doi:10.1093/ajcn/40.1.48.

[S15] D. Marthinsen and S. E. Fleming. Excretion of Breath and Flatus Gases by Humans Consuming High-Fiber Diets. *Journal of Nutrition*, 112(6):1133–1143, 1982. doi:10.1093/jn/112.6.1133.

[S16] C. A. Hickey, D. H. Calloway, and E. L. Murphy. Intestinal gas production following ingestion of fruits and fruit juices. *The American Journal of Digestive Diseases*, 17(5): 383–388, 1972. doi:10.1007/BF02231287.

[S17] M. D. Levitt, R. B. Lasser, J. S. Schwartz, and J. H. Bond. Studies of a Flatulent Patient. *New England Journal of Medicine*, 295(5):260–262, 1976. doi:10.1056/NEJM197607292950507.

[S18] E. Kirk. The Quantity and Composition of Human Colonic Flatus. *Gastroenterology*, 12 (5):782–794, 1949. doi:10.1016/s0016-5085(49)80154-5.

[S19] C. Rønholt, O. Ø. Rasmussen, and J. Christiansen. Ambulatory manometric recording of anorectal activity. *Diseases of the Colon & Rectum*, 42(12):1551–1559, 1999. doi:10.1007/bf02236205.

[S20] M. Corsetti, G. Pagliaro, I. Demedts, E. Deloose, A. Gevers, C. Scheerens, N. Rommel, and J. F. Tack. Pan-Colonic Pressurizations Associated With Relaxation of the Anal Sphincter in Health and Disease: A New Colonic Motor Pattern Identified Using High-Resolution Manometry. *The American Journal of Gastroenterology*, 112(3):479–489, 2017. doi:10.1038/ajg.2016.341.

[S21] F. Luft, L. V. Fynne, H. N. Gregersen, F. H. Lundager, S. Buntzen, L. Lundby, S. Laurberg, and K. Krogh. Functional luminal imaging probe: a new technique for dynamic evaluation of mechanical properties of the anal canal. *Techniques in Coloproctology*, 16 (6):451–457, 2012. doi:10.1007/s10151-012-0871-0.

[S22] G. Sørensen, D. Liao, L. Lundby, L. V. Fynne, S. Buntzen, H. N. Gregersen, S. Laurberg, and K. Krogh. Distensibility of the anal canal in patients with idiopathic fecal incontinence: a study with the Functional Lumen Imaging Probe. *Neurogastroenterology & Motility*, 26 (2):255–263, 2014. doi:10.1111/nmo.12258.

[S23] R. C. Miller, G. T. R. Lewis, D. C. C. Bartolo, F. Cerveró, and N. J. M. Mortensen. Sensory discrimination and dynamic activity in the anorectum: Evidence using a new ambulatory technique. *British Journal of Surgery*, 75(10):1003–1007, 1988. doi:10.1002/bjs.1800751018.

[S24] K. Nagai, S. Iwata, A. Takasu, M. Miwa, Y. Ohtsu, K. Takeuchi, M. Ochi, and M. Takeuchi. Aerodynamic Study of Esophageal Speech. *Practica Oto-Rhino-Laryngologica, Supplement*, 1993(Supplement65):164–170, 1993. doi:10.5631/jibirinsuppl1986.1993.supplement65_164.

[S25] W. Grolman, S. E. J. Eerenstein, F. M. L. Tan, R. A. Tange, and P. F. Schouwenburg. Aerodynamic and Sound Intensity Measurements in Tracheoesophageal Voice. *ORL*, 69 (2):68–76, 2007. doi:10.1159/000097401.

[S26] M. L. Ng. Aerodynamic characteristics associated with oesophageal and tracheoesophageal speech of Cantonese. *International Journal of Speech-Language Pathology*, 13(2):137–144, 2011. doi:10.3109/17549507.2011.534176.

[S27] R. Mattéoli, J. Gilbert, C. Vergez, J. Dalmont, S. Maugeais, S. Terrien, and F. Ablitzer. Minimal blowing pressure allowing periodic oscillations in a model of bass brass instruments. *Acta Acustica*, 5:57, 2021. doi:10.1051/aacus/2021049.

[S28] J. Robbins, H. B. Fisher, E. C. Blom, and M. I. Singer. A Comparative Acoustic Study of Normal, Esophageal, and Tracheoesophageal Speech Production. *Journal of Speech and Hearing Disorders*, 49(2):202–210, 1984. doi:10.1044/jshd.4902.202.

[S29] R. H. Pindzola and B. H. Cain. Duration and Frequency Characteristics of Tracheoesophageal Speech. *Annals of Otology Rhinology & Laryngology*, 98(12):960–964, 1989. doi:10.1177/000348948909801208.

[S30] D. G. Deschler, E. T. Doherty, C. G. Reed, and M. I. Singer. Effects of sound pressure levels on fundamental frequency in tracheoesophageal speakers. *Otolaryngology - Head and Neck Surgery*, 121(1):23–26, 1999. doi:10.1016/s0194-5998(99)70117-8.

[S31] M. Chervinsky. Malacoda. Blog post, flatology.com; not peer reviewed (accessed 1 November 2026), 2021. URL https://flatology.com/malacoda/.

[S32] ISO. *ISO 226:2023 Acoustics - Normal equal-loudness-level contours*. International Organization for Standardization, Geneva, 3 edition, 2023.

[S33] J. E. Hawkins and S. S. Stevens. The masking of pure tones and of speech by white noise. *Journal of the Acoustical Society of America*, 22(1):6–13, 1950. doi:10.1121/1.1906581.

[S34] D. Kumar, D. J. Waldron, N. S. Williams, C. Browning, M. R. E. Hutton, and D. L. Wingate. Prolonged anorectal manometry and external anal sphincter electromyography in ambulant human subjects. *Digestive Diseases and Sciences*, 35(5):641–648, 1990. doi:10.1007/bf01540414.

[S35] D. Licina, J. Pantelic, A. Melikov, C. Sekhar, and K. W. Tham. Experimental investigation of the human convective boundary layer in a quiescent indoor environment. *Building and Environment*, 75:79–91, 2014. doi:10.1016/j.buildenv.2014.01.016.

[S36] D. Licina, Y. Tian, and W. W. Nazaroff. Inhalation intake fraction of particulate matter from localized indoor emissions. *Building and Environment*, 123:14–22, 2017. doi:10.1016/j.buildenv.2017.06.037.

[S37] B. W. Olesen. European standardisation on indoor air quality. *REHVA Journal*, (6):12–16, 2024. URL https://www.rehva.eu/rehva-journal/chapter/european-standardisation-on-indoor-air-quality.

[S38] G. R. Gibson, G. T. Macfarlane, and J. H. Cummings. Sulphate reducing bacteria and hydrogen metabolism in the human large intestine. *Gut*, 34:437–439, 1993. doi:10.1136/gut.34.4.437.

[S39] D. J. Braccia, X. Jiang, M. Pop, et al. The Capacity to Produce Hydrogen Sulfide (H2S) via Cysteine Degradation Is Ubiquitous in the Human Gut Microbiome. *Frontiers in Microbiology*, 12:705583, 2021. doi:10.3389/fmicb.2021.705583.

[S40] G. R. Gibson, S. Macfarlane, and G. Macfarlane. Metabolic interactions involving sulphate-reducing and methanogenic bacteria in the human large intestine. *FEMS Microbiology Ecology*, 12(2):117–125, 1993. doi:10.1016/0168-6496(93)90006-S.

[S41] A. Strocchi, J. K. Furne, C. J. Ellis, and M. D. Levitt. Competition for hydrogen by human faecal bacteria: evidence for the predominance of methane producing bacteria. *Gut*, 32(12):1498–1501, 1991. doi:10.1136/gut.32.12.1498.

[S42] T. H. Florin. Hydrogen sulphide and total acid-volatile sulphide in faeces, determined with a direct spectrophotometric method. *Clinica Chimica Acta*, 196(2-3):127–134, 1991. doi:10.1016/0009-8981(91)90065-K.

[S43] J. Levine, C. J. Ellis, J. K. Furne, J. R. Springfield, and M. D. Levitt. Fecal Hydrogen Sulfide Production in Ulcerative Colitis. *The American Journal of Gastroenterology*, 93 (1):83–87, 1998. doi:10.1111/j.1572-0241.1998.083_c.x.

[S44] A. Strocchi, J. K. Furne, C. Ellis, and M. D. Levitt. Methanogens outcompete sulphate reducing bacteria for H2 in the human colon. *Gut*, 35(8):1098–1101, 1994. doi:10.1136/gut.35.8.1098.

[S45] M. D. Levitt, J. K. Furne, J. R. Springfield, et al. Detoxification of hydrogen sulfide and methanethiol in the cecal mucosa. *Journal of Clinical Investigation*, 104:1107–1114, 1999. doi:10.1172/JCI7712.

[S46] R. Picton, M. C. Eggo, G. A. Merrill, et al. Mucosal protection against sulphide: importance of the enzyme rhodanese. *Gut*, 50:201–205, 2002. doi:10.1136/gut.50.2.201.

[S47] A. Pol, G. H. Renkema, A. Tangerman, et al. Mutations in SELENBP1, encoding a novel human methanethiol oxidase, cause extraoral halitosis. *Nature Genetics*, 50:120–129, 2018. doi:10.1038/s41588-017-0006-7.

[S48] E. A. Magee, C. J. Richardson, R. Hughes, et al. Contribution of dietary protein to sulfide production in the large intestine: an in vitro and a controlled feeding study in humans. *American Journal of Clinical Nutrition*, 72:1488–1494, 2000. doi:10.1093/ajcn/72.6.1488.

[S49] M. D. Levitt, J. R. Springfield, J. K. Furne, T. W. Koenig, and F. L. Suarez. Physiology of sulfide in the rat colon: use of bismuth to assess colonic sulfide production. *Journal of Applied Physiology*, 92(4):1655–1660, 2002. doi:10.1152/japplphysiol.00907.2001.

[S50] L. M. Teigen, P. P. Mathai, S. Lopez, et al. Differential hydrogen sulfide production by a human cohort in response to animal- and plant-based diet interventions. *Clinical Nutrition*, 41:1153–1162, 2022. doi:10.1016/j.clnu.2022.03.028.

[S51] C. K. Yao, A. Rotbart, J. Z. Ou, K. Kalantar-Zadeh, J. G. Muir, and P. R. Gibson. Modulation of colonic hydrogen sulfide production by diet and mesalazine utilizing a novel gas-profiling technology. *Gut Microbes*, 9(6):510–522, 2018. doi:10.1080/19490976.2018.1451280.

[S52] S. U. Christl, G. R. Gibson, and J. H. Cummings. Role of dietary sulphate in the regulation of methanogenesis in the human large intestine. *Gut*, 33(9):1234–1238, 1992. doi:10.1136/gut.33.9.1234.

[S53] G. K. Grimble. Fibre, fermentation, flora, and flatus. *Gut*, 30(1):6–13, 1989. doi:10.1136/gut.30.1.6.

[S54] F. L. Suarez, J. K. Furne, J. Springfield, and M. D. Levitt. Bismuth subsalicylate markedly decreases hydrogen sulfide release in the human colon. *Gastroenterology*, 114(5):923–929, 1998. doi:10.1016/S0016-5085(98)70311-7.

[S55] C. J. Giffard, S. B. Collins, N. C. Stoodley, R. F. Butterwick, and R. M. Batt. Administration of charcoal, Yucca schidigera, and zinc acetate to reduce malodorous flatulence in dogs. *Journal of the American Veterinary Medical Association*, 218(6):892–896, 2001. doi:10.2460/javma.2001.218.892.

[S56] S. Li, L. Ahmed, R. Zhang, et al. Smelling Sulfur: Copper and Silver Regulate the Response of Human Odorant Receptor OR2T11 to Low-Molecular-Weight Thiols. *Journal of the American Chemical Society*, 138:13281–13288, 2016. doi:10.1021/jacs.6b06983.

[S57] E. Block, V. S. Batista, H. Matsunami, et al. The role of metals in mammalian olfaction of low molecular weight organosulfur compounds. *Natural Product Reports*, 34:529–557, 2017. doi:10.1039/c7np00016b.

[S58] X. F. Duan, E. Block, Z. Li, et al. Crucial role of copper in detection of metal-coordinating odorants. *Proceedings of the National Academy of Sciences*, 109:3492–3497, 2012. doi:10.1073/pnas.1111297109.

[S59] F. Haag, L. Ahmed, K. M. Reiss, et al. Copper-mediated thiol potentiation and mutagenesis-guided modeling suggest a highly conserved copper-binding motif in human OR2M3. *Cellular and Molecular Life Sciences*, 77(11):2157–2179, 2020. doi:10.1007/s00018-019-03279-y.

[S60] R. Zhang, Y. Pan, L. Ahmed, et al. A Multispecific Investigation of the Metal Effect in Mammalian Odorant Receptors for Sulfur-Containing Compounds. *Chemical Senses*, 43: 357–366, 2018. doi:10.1093/chemse/bjy022.